*Sādhanā* (2021)46:107
https://doi.org/10.1007/s12046-021-01625-0


# Nonlocal and surface effects on the bending analysis of flexoelectrically actuated piezoelectric microbeams in hygrothermal environment

FARZAD EBRAHIMI[1,*], MAHSA KARIMIASL[1] and VINYAS MAHESH[2]

[1]Department of Mechanical Engineering, Faculty of Engineering, Imam Khomeini International University, Qazvin, Iran
[2]Department of Aerospace Engineering, Indian Institute of Science, Bangalore, India
e-mail: febrahimy@eng.ikiu.ac.ir

MS received 25 February 2019; revised 23 October 2019; accepted 24 October 2019

**Abstract.** In this article, the bending analysis of flexoelectric functionally graded (FG) microbeams according to nonlocal elasticity theory is verified. To this end, higher order refined beam theory has been used. The foundation of FG microbeam includes Winkler-Pasternak layer. Hamilton's principle is used to obtain the governing equations based on the nonlocal theory and solved employing an analytical solution. The model is designed in such a way that the properties change continuously. A parametric study is presented to inquire the nonlocal parameter, power-law hygro-thermal-loadings, flexoelectric effect, transverse external loading, on the bending characteristics of FG microbeam. It is found that boundary conditions, flexoelectric effect, nonlocal parameter, power-law index and beam geometrical parameters have notable effects on dimensionless deflection of FG microscale beams.

**Keywords.** Bending; Microbeam; Hygro-thermal loading; Winkler-Pasternak foundation; Nonlocal elasticity theory.

## 1. Introduction

Functionally graded material (FGM) is one of the materials that exhibit different properties in different regions due to the gradual change in the chemical composition, distribution, orientation, or size of the reinforcing phase in one or more dimensions. This gradual change in the structure and properties has led to the expansion of the use of these materials. Considering the various applications of these materials in the air, military and defense industries, the study of methods and techniques for making these materials is important and necessary. Therefore, the hygro-thermal analysis of FGM structures is a benefit case in research. The nonlocal continuum mechanics theories in contrast to classical theory emphasize that the stress at a point is not just directed to a point, but also depends on other points. Meanwhile, in the classical theory, stress is limited to a single point as expressed by Eringen [1, 2]. Following the Eringen's theory, many studies have been carried out to highlight some of the important issues. The postbuckling analysis of FG beams in microscales under thermal loading was investigated by Ansari *et al* [3]. The buckling behaviour of piezoelectric FG beams under thermal and electric loading was studied by Kiani *et al* [4]. Rahmani and Jandaghian [5] researched the mechanical response of FG beam theory through third-order shear deformation via nonlocal theory. Yang *et al* [6] studied the nonlinear vibration of single walled carbon nanotubes (SWCNTs). Based on the elastic medium, the stability responses of SWCNT were described. The effect of Winkler and Pasternak parameter, aspect ratio of the SWCNT and nonlocal parameter were also studied in their research. The vibration and buckling characteristics of piezoelectric and piezomagnetic nanobeams based on various beam models were verified by Ebrahimi and Barati [7–11]. In their research, the electro-magnetic effect of piezoelectric materials has been investigated and also the mechanical responses of FGM nanobeams have been observed under various significant parameters. They realized that the effect of the electro-magnetic hygro-thermal loading increases the dimensionless frequency and buckling load. The vibration, buckling and bending behaviour of Timoshenko nanobeams based on meshless method was investigated by Roque *et al* [12]. Embedded in the nonlocal component relevance of Eringen, the majority of articles were published searching to extend the nonlocal beam models for nano structures. Peddieson *et al* [13] proposed nonlocal Euler–Bernoulli and Timoshenko beam theory whose credibility to predict bending behaviour was accepted and verified by many studies [14–16]. During the years of research the small-size effects in SWCNTs were studied by Murmu and Pradhan [17]. Thermo-magneto-electro-elastic analysis of a

*For correspondence
Published online: 25 May 2021

functionally graded nanobeam integrated with functionally graded piezo magnetic layers was studied by Arefi [18]. Sobhy and Zenkour studied the thermal buckling analysis of single-layered graphene sheets lying on an elastic medium [19]. Bending of electro-mechanical sandwich nanoplate based on silica Aerogel foundation was examined by Ghorbanpour *et al* [20]. The influence of parameters such as applied voltage, porosity index, foundation parameter, aspect ratio on the bending response of sandwich nanoplates was studied. Simsek *et al* [21] presented the bending analysis of shear and normal deformations beam theory based on nonlocal theory. 22] assessed the structural stability response of FGM and Carbon Nano-Tube (CNT) reinforced composite plates and curved panels. It was revealed from the evaluation that the geometrical parameters as well as material parameters such as power-law index, distribution of carbon nanotubes have a significant influence. Adapting First-order Shear Deformation Theory (FSDT), the dynamic response of moderately thick FGM conical, cylindrical shells and annular plates was probed by Tornabene *et al* [23]. A similar investigation was also reported by Tornabene *et al* [24] dealing with dynamic analysis of FGM and laminated doubly curved shells and panels of revolution with a free-form meridian. The forced vibration characteristics of functionally graded carbon nanotubes-reinforced composite (FG-CNTRC) shell structures have been studied thoroughly in [25]. This study emphasized on the effect of boundary conditions and geometrical parameters on the dynamic behaviour of FG-CNTRC shells (Table 1). The influence of external thermal environment on the stability characteristics of FGM plates and cylindrical shells was evaluated incorporating modified FSDT [26]. Considering the Generalized Differential Quadrature (GDQ) method, the bending response of FGM and laminated doubly-curved shells and panels was probed by Tornabene *et al* [27] via FSDT. In this study, the influence of nonlinear and linear elastic foundations was highlighted. In the article [28], the variation of stresses across the thickness of FG doubly-curved sandwich shell structures and shells of revolution was demonstrated employing the generalized zigzag displacement field and the Carrera Unified Formulation (CUF). The effect of Carbon Nanotubes (CNT) agglomeration on the free vibrations of laminated composite doubly-curved shells and panels reinforced by CNTs [29].

In this article, the bending behaviour of nanobeams under hygro-thermal and transverse external loading has been researched based on refined shear deformable theory. The governing equations are derived by the Hamilton principle and are solved via analytical method. The effect of several parameters such as flexoelectric effect, nonlocal parameter, hygro-thermal loading, different boundary conditions, power-law index and Winkler-Pasternak foundation on bending response has been investigated.

**Table 1.** The admissible functions $X_m(x)$ [31].

| | BC | The functions $X_m$ |
|---|---|---|
| | At $x$=0, $a$ | $X_m(x)$ |
| SS | $X_m(0) = X''_m(0) = 0$ | $Sin(\alpha x)$ |
| | $X_m(a) = X''_m(a) = 0$ | |
| CC | $X_m(0) = X'_m(0) = 0$ | $Sin^2(\alpha x)$ |
| | $X_m(a) = X'_m(a) = 0$ | |

## 2. Theory and formulation

### 2.1 *The properties of P-FGM microbeam*

The functionally graded microbeam resting on elastic foundation is shown in figure 1. First moment to Young's modulus being zero by satisfying the exact locality of neutral axis which shown as follows:

$$\int_{-h/2}^{h/2} E(z_{ms})(z_{ms} - h_0)dz_{ms} = 0 \tag{1}$$

$z$=$h_0$ is shown by

$$h_0 = \frac{\int_{-h/2}^{h/2} E(z_{ms})\, z_{ms} dz_{ms}}{\int_{-h/2}^{h/2} E(z_{ms})\, dz_{ms}} \tag{2}$$

FG microbeam based on elastic medium foundation with width $b$, length $L$, and thickness $h$ was considered that its coordinates is illustrated in figure 1. $E$, $\rho$, $\alpha$ and $\beta$ are Young's modulus, mass density, thermal expansion and moisture expansion coefficient and the nonlocal hygro-thermal material properties can be represented by

$$E(z_{ns}) = (E_c - E_m)\left(\frac{z_{ns} + h_0}{h} + \frac{1}{2}\right)^p + E_m, \tag{3a}$$

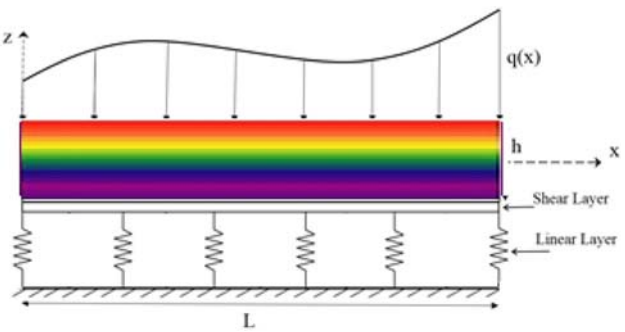


**Figure 1.** Geometry of functionally graded microbeam resting on elastic foundation.

$$\rho(z_{ns}) = (\rho_c - \rho_m)\left(\frac{z_{ns}+h_0}{h}+\frac{1}{2}\right)^p + \rho_m, \tag{3b}$$

$$\alpha(z_{ns}) = (\alpha_c - \alpha_m)\left(\frac{z_{ns}+h_0}{h}+\frac{1}{2}\right)^p + \alpha_m, \tag{3c}$$

$$\beta(z_{ns}) = (\beta_c - \beta_m)\left(\frac{z_{ns}+h_0}{h}+\frac{1}{2}\right)^p + \beta_m, \tag{3d}$$

$p$ is the distribution of material properties across the thickness are investigated by Power-law exponent. So, the temperature-dependent material coefficients [30] expressed by

$$P = P_0(P_{-1}\,T^{-1} + 1 + P_1\,T + P_2\,T^2 + P_3\,T^3) \tag{4}$$

The coefficients of material phases expressed by $P_0, P_{-1}, P_1, P_2$ and $P_3$.

## 2.2 *Kinematic relations*

The displacement fields of FG microbeam using refined shear deformable beam theory can be illustrated by

$$\mathrm{u_x(x,z) = u(x) - z\frac{\partial w_b}{\partial x} - f(z)\frac{\partial w_s}{\partial x}}, \tag{5}$$

$$\mathrm{u_z(x,z) = w_b(x) + w_s(x)} \tag{6}$$

where axial mid-plane displacement is defined by $u$ and $w_s$ and $w_b$ are the shear and bending components of displacement, respectively. The shape function $f$(z) represents the shear stress/strain distribution across the beam thickness.

$$f(z) = z - \frac{H}{\pi}sin\left[\frac{\pi z}{H}\right] \tag{7}$$

The strains of the beam model illustrate as follows:

$$\varepsilon_{xx} = \frac{\partial u}{\partial x} - z\frac{\partial^2 w_b}{\partial x^2} - f(z)\frac{\partial^2 w_s}{\partial x^2}, \tag{8}$$

$$\gamma_{xz} = g(z)\frac{\partial w_s}{\partial x} \tag{9}$$

where g(z)=1−df(z)/dz.

The constitutive relation of the multiscale composite shell can be expressed as

$$\begin{Bmatrix}\sigma^n_{xx}\\ \sigma^n_{yy}\\ \sigma^n_{xy}\end{Bmatrix} = \begin{bmatrix}Q_{11} & 0 & 0\\ 0 & Q_{22} & 0\\ 0 & 0 & Q_{12}\end{bmatrix}\begin{Bmatrix}\varepsilon^n_{xx}\\ \varepsilon^n_{yy}\\ \varepsilon^n_{zz}\end{Bmatrix} \tag{10}$$

The reduce stiffness modulus of FG microbeam can be expressed by

$$Q_{11} = Q_{22} = \frac{E}{1-\nu^2}, Q_{12} = G \tag{11}$$

Hamilton's principle expressed by

$$\int_0^t \delta(\Pi_S + \Pi_W)\mathrm{d}t = 0 \tag{12}$$

where $\Pi_S$ is the total strain energy and external applied forces denote by $\Pi_W$. The strain energy variation $\Pi_S$ can be computed as

$$\delta\Pi_S = \int \sigma_{ij}\delta\varepsilon_{ij}dv = \int \sigma_x\delta\varepsilon_x + \sigma_{xz}\delta\gamma_{xz} \tag{13}$$

With substitute Eqs.(5)–(7) into Eq. (9):

$$\delta\Pi_S = \int_0^l (N\frac{\partial\delta u}{\partial x} - M_b\frac{\partial^2\delta w_b}{\partial x^2} - M_s\frac{\partial^2\delta w_s}{\partial x^2} + Q\frac{\partial\delta w_s}{\partial x})dx \tag{14}$$

$N$ is forces and $M_b, M_s$ and $Q$ moments equation are illustrated as follows:

$$\begin{aligned}(N, M_b, M_s) &= \int_A (1, z, f)\sigma_i dA, i = (x, y, xy),\\ Q_i &= \int_A g\sigma_i dA, i = (xz, yz)\end{aligned} \tag{15}$$

The work done of applied forces of first variation can be expressed by:

$$\begin{aligned}\delta\Pi_w = \int_0^a [(-N_x^0\frac{\partial w^b}{\partial x}\frac{\partial\delta w^b}{\delta x} - k_w\delta(w^b + w^s)\\ + k_p\partial^2\frac{(w_{b+}w_s)}{\partial x^2}]dx + f_{13}\delta(w^b + w^s)\end{aligned} \tag{16}$$

where $k_w$, $k_p$ and $f_{13}$ are linear, shear and flexoelectric coefficients, respectively. And in above relations $N_x^0 = N^T + N^H$:

$$N^T = \int_{-h/2-h_0}^{\frac{h}{2}-h_0} (\alpha\Delta T)dz, \tag{17a}$$

$$N^H = b\int_{-h/2-h_0}^{\frac{h}{2}-h_0} (\beta\Delta H)dz \tag{17b}$$

where $\Delta T = T - T_0$, $T_0$ is the reference temperature concentration; $\Delta H = H - H_0$, $H_0$ is the reference moisture concentration.

By inserting Eqs. (11)–(14) in Eq. (10) when the coefficients of $\delta u, \delta w_b$ and $\delta w_s$ are equal to zero, governing equations are obtained as follows:

$$\frac{\partial N}{\partial x} = 0, \tag{18a}$$

$$\frac{\partial^2 M_b}{\partial x^2} + \left(-N^T - N^H + K_p\right)\nabla^2\left(w^b + w^s\right) + k_w\left(w^b + w^s\right) + f_{13}\delta\left(w^b + w^s\right) = 0, \tag{18b}$$

$$\frac{\partial^2 M_s}{\partial x^2} + \frac{\partial Q}{\partial x} + \left(-N^T - N^H\right)\frac{\partial^2\left(w^b + w^s\right)}{\partial x} - K_p\frac{\partial^2\left(w^b + w^s\right)}{\partial x} + k_w\left(w^b + w^s\right) + f_{13}\delta\left(w^b + w^s\right) = 0 \tag{18c}$$

### 2.3 *Theory of nonlocal elasticity*

Nonlocal elasticity theory mentions that the nonlocal stress tensor at a reference point relies not only on the strain tensor of the same coordinate but also on another point in the solid. For a nonlocal magneto-electro-elastic plate the basic equations may be defined as

$$\sigma_{ij} = \int_V \alpha(|x' - x|, \tau)\left[C_{ijkl}\varepsilon_{kl}(x') - e_{mij}E_m(x') - q_{nij}H_n(x')\right]dV(x'), \tag{19a}$$

$$D_i = \int_V \alpha(|x' - x|, \tau)[e_{ikl}\varepsilon_{kl}(x') + s_{im}E_m(x') + d_{in}H_n(x')]dV(x'), \tag{19b}$$

$$B_i = \int_V \alpha(|x' - x|, \tau)[q_{ikl}\varepsilon_{kl}(x') + d_{im}E_m(x') + \chi_{in}H_n(x')]dV(x') \tag{19c}$$

in which $\sigma_{ij}, D_i, B_i$ denote the components of stress, electric displacement and magnetic induction, $\varepsilon_{kl}, E_m$ and $H_n$ are the components of linear strain, electric field and magnetic field. Additionally,$C_{ijkl}$,$s_{im}$ and $\chi_{in}$ are the components of elastic stiffness, dielectric permittivity and magnetic permittivity coefficients. Finally, $e_{mij}, q_{nij}$, and $d_{in}$ are the piezoelectric, piezo-magnetic, and magneto-electric-elastic coefficients, respectively. $\alpha(|x' - x|, \tau)$ is the nonlocal kernel function and $|x' - x|$ is the Euclidean distance. $\tau = e_0 a/l$ is defined as scale coefficient, where $e_0$ is a material constant which is determined experimentally or approximated by matching the dispersion curves of plane waves with those of atomic lattice dynamics; and $a$ and $l$ are the internal and external characteristic length of the microstructures, respectively.

As well as:

$$\sigma_{ij-}(ea)^2\nabla^2\sigma_{ij} = \left[C_{ijkl}\varepsilon_{kl} - f_{klij}\frac{\partial_{E_K}}{\partial x_l} + C_{ijkl}\alpha_{kl}\Delta T - C_{ijkl}\beta_{kl}\Delta H\right] \tag{20}$$

where $\beta_{ij}$ and $\alpha_{ij}$ are moisture and thermal expansion coefficients.

Where the cross-sectional rigidities are calculated:

$$\left(1 - \mu^2\nabla^2\right)N = A\frac{\partial u}{\partial x} - B\frac{\partial^2 w}{\partial x^2} - B_s\frac{\partial^2 w}{\partial x^2}, \tag{21}$$

$$\left(1 - \mu^2\nabla^2\right)M_b = B\frac{\partial u}{\partial x} - D\frac{\partial^2 w}{\partial x^2} + D_s\frac{\partial^2 w}{\partial x^2}, \tag{22}$$

$$\left(1 - \mu^2\nabla^2\right)M_s = \left(B_s\frac{\partial^3 u}{\partial x^3} - D_S\frac{\partial^4 w_b}{\partial x^4} - H_S\frac{\partial^4 w_b}{\partial x^4}\right), \tag{23}$$

$$\{A, B, B_S, D, D_S, H_S\} = \int_{-\frac{h}{2}}^{\frac{h}{2}} c11\left(1, z, f, z^2, fz, f^2\right)dz \tag{24}$$

Now, by substituting Eqs. (17) and (18), (19) in Eqs. (22) and (23), (24) the explicit equations bending moment can be expressed as follows:

$$\frac{\partial N}{\partial x} = \left(A\frac{\partial^2 u}{\partial x^2} - B\frac{\partial^3 w_b}{\partial x^3} - B_S\frac{\partial^3 w_s}{\partial x^3}\right), \tag{25}$$

$$\frac{\partial^2 M_b}{\partial x^2} = \left(B\frac{\partial^3 u}{\partial x^3} - D\frac{\partial^4 w_b}{\partial x^4} - D_S\frac{\partial^4 w_s}{\partial x^4}\right) + k_p\frac{\partial^2\left(w^b + w^s\right)}{\partial x} - k_w\left(w^b + w^s\right) - \mu\left(-N^T - N^H\right)\frac{\partial^2\left(w^b + w^s\right)}{\partial x} + k_p\frac{\partial^2\left(w^b + w^s\right)}{\partial x} - k_w\left(w^b + w^s\right) - \frac{e_{31}}{2k_{33}}(f_{13}), \tag{26}$$

$$\frac{\partial^2 M_s}{\partial x^2} + \frac{\partial Q}{\partial x} = \left(B_s\frac{\partial^3 u}{\partial x^3} - D_S\frac{\partial^4 w_b}{\partial x^4} - H_S\frac{\partial^4 w_b}{\partial x^4}\right) + k_p\frac{\partial^2\left(w^b + w^s\right)}{\partial x^2} - k_w\left(w^b + w^s\right) - \mu(-N^T - N^H)\frac{\partial^2\left(w^b + w^s\right)}{\partial x} + k_p\frac{\partial^2\left(w^b + w^s\right)}{\partial x} - k_w\left(w^b + w^s\right) - \frac{e_{31}}{2k_{33}}(f_{13}) \tag{27}$$

## 3. Solution procedure

In this section, an analytical solution is performed in which the generalized displacements are expanded in a double Fourier series in terms of unknown parameters. The selection of the functions in these series is associated with those which satisfy the boundary edges of the microplate. These boundary edges are given as

- Simply-supported (S):

$$w_b = w_s = N_x = M_x = 0 \quad \text{at x} = 0,\ \text{a} \tag{28}$$

- Clamped (C):

$$u = w_b = w_s = 0 \quad \text{at x} = 0, \text{a} \tag{29}$$

To obtain boundary conditions, we use the following equations:

$$u = \sum_{n=1}^{\infty} U_n \frac{\partial X_n(x)}{\partial x} e^{i\omega_n t}, \tag{30}$$

$$w_b = \sum_{n=1}^{\infty} W_{bn} X_n(x) e^{i\omega_n t}, \tag{31}$$

$$w_s = \sum_{n=1}^{\infty} W_{sn} X_n(x) e^{i\omega_n t} \tag{32}$$

where ($U_{mn}$,$W_{bmn}$, $W_{zmn}$) are the unknown coefficients and for various boundary conditions (BC).

Where:

$$[K]\begin{Bmatrix} u_n \\ w_{bn} \\ w_{sn} \end{Bmatrix} = \begin{Bmatrix} 0 \\ Q_n(1+\mu\frac{n^2\pi^2}{L^2}) \\ Q_n\left(1+\mu\frac{n^2\pi^2}{L^2}\right) \end{Bmatrix} \tag{33}$$

Where [K], [F] are the stiffness, loading matrixes for microbeam, respectively.

$$\begin{aligned}
&k_{1,1} = A\alpha_1, \quad K_{1,2} = B\alpha_2, \quad K_{1,3} = B_s\alpha_2,\\
&K_{2,1} = B\alpha_{11}, k_{2,2} = D\alpha_7 + k_1\alpha_5 - k_p\alpha_6\\
&+ \mu[(-N^T - N^H + k_2)\alpha_6 - (\left(k_1 + \frac{e_{31}}{2k_{33}})f_{13}\right)\alpha_5],\\
&K_{2,3} = D_s\alpha_7 + k_1\alpha_5 - k_p\alpha_6 + \mu[(-N^T - N^H + k_2)\alpha_6\\
&- (\left(k_1 + \frac{e_{31}}{2k_{33}})f_{13}\right)\alpha_5]\\
&K_{3,1} = B_s\alpha_1, K_{3,2} = D_s\alpha_7 + k_w\alpha_5 - k_2\alpha_6\\
&+ \mu[(-N^T - N^H + k_2)\alpha_6 - (\left(k_1 + \frac{e_{31}}{2k_{33}})f_{13}\right)\alpha_5],\\
&K_{3,3} = H_s\alpha_7 + k_1\alpha_5 - k_2\alpha_6 + (-N^T - N^H + k_2)\alpha_6\\
&- (\left(k_1 + \frac{e_{31}}{2k_{33}})f_{13}\right)\alpha_5
\end{aligned}$$

$$\begin{aligned}
F_{1,1} &= N\alpha_3,\\
F_{2,2} &= M_b(1-\mu\alpha_6),\\
F_{3,3} &= M_s(1-\mu\alpha_6) + Q(1-\mu\alpha_3)
\end{aligned} \tag{34}$$

In which

$$\begin{aligned}
&\alpha_1 = \int_0^a X'(x)X''(x)dx, \quad \alpha_2 = \int_0^a X(x)X'''(x)dx,\\
&\alpha_7 = \int_0^a X(x)X''''(x)dx,\\
&\alpha_5 = \int_0^a X(x)X(x)dx, \quad \alpha_3 = \int_0^a X(x)X'(x)dx,\\
&\alpha_{11} = \int_0^a X'(x)X'''(x)dx,\\
&\alpha_6 = \int_0^a X(x)X''(x)dx
\end{aligned} \tag{35}$$

The uniform load is supposed that leading to bending and is illustrated by equations below :

$$q = \sum_{n=1}^{\infty} Q_n \sin[\frac{n\pi}{L}x]\sin\omega t, \tag{36}$$

$$Q_n = \frac{2}{L}\int_{x_0-c}^{x_0+c} \sin[\frac{n\pi}{L}x]q_x dx \tag{37}$$

Fourier coefficients ($Q$n) and the uniform load ($q$(x) = $q$0) and the centroid coordinates ( x0). Also, the harmonic load relation intensity can be expressed as:

$$q(x) = P\delta(x - x_0)\sin\omega t, \tag{38}$$

$$Q_n = \frac{2P}{L}\sin\left[\frac{n\pi}{L}x_0\right] \tag{39}$$

In which δ is the Dirac delta.

## 4. Numerical results and discussions

This section studies the bending behaviour of FG microbeam through a higher order refined theory and trigonometric function. The material properties tabulated in table 2 for a P-FGM microbeam that including of metal (SUS 304) at $z = -h/2$ with $\beta_m = 0.0005$ and ceramic ($Si_3N_4$), at $z$=+$h$/2 with $\beta_c = 0$[24] are considered for evaluation. The credibility of the present work is verified by comparing the results from the proposed formulation of this work with those reported by [25]. As depicted in table 3, there exists a close agreement between the dimensionless deflection obtained from the proposed model and those mentioned in [25].

In this regard, the dimensionless deflections are adopted as

**Table 2.** Temperature-dependent material properties of FGMs [32].

| Material | Properties | $P_0$ | $P_{-1}$ | $P_1$ | $P_2$ | $P_3$ |
|---|---|---|---|---|---|---|
| $Si_3N_4$ | $E$(Pa) | 348.43e+9 | 0 | −3.070e−4 | 2.160e−7 | −8.946e−11 |
| | $\alpha(K^{-1})$ | 5.8723e−6 | 0 | 9.095e−4 | 0 | 0 |
| | $\rho(Kg/m^3)$ | 2370 | 0 | 0 | 0 | 0 |
| | $v$ | 0.24 | 0 | 0 | 0 | 0 |
| SUS 304 | $E$(Pa) | 201.04e+9 | 0 | 3.079e−4 | −6.534e−7 | 0 |
| | $\alpha(K^{-1})$ | 12.330e−6 | 0 | 8.086e−4 | 0 | 0 |
| | $\rho(Kg/m^3)$ | 8166 | 0 | 0 | 0 | 0 |
| | $v$ | 0.3262 | 0 | −2.002e−4 | 3.797e−7 | 0 |

**Table 3.** The show of dimensionless deflections of FG microbeams with different beam theory.

| L/h | μ(nm2) | EBT [33] | TBT [33] | RBT [33] | RBT Present |
|---|---|---|---|---|---|
| | 1 | 1.5674 | 1.5673 | 1.5674 | 1.8092 |
| | 2 | 1.7028 | 1.7027 | 1.7028 | 1.9832 |
| | 3 | 1.8381 | 1.8381 | 1.8382 | 2.1163 |
| | 4 | 1.9734 | 1.9735 | 2.9736 | 3.2310 |
| 10 | 1 | 1.4622 | 1.4622 | 1.4622 | 1.7821 |
| | 2 | 1.5898 | 1.5898 | 1.5898 | 1.8014 |
| | 3 | 1.7173 | 1.7174 | 1.7174 | 1.9201 |
| | 4 | 1.8489 | 1.8450 | 1.8450 | 2.0915 |

$$W = 100\frac{C_{11}I}{q_0L^4} \tag{40}$$

In figure 2, the influence of the material gradient index on the dimensionless deflections of FG microbeam is analysed considering different nonlocal parameters. To this end, the parameters were set to L/h = 10, $\Delta T$ = 20, $\Delta H$ = 1, $K_w$= $K_p$=20. It is found that as the material gradient index increases the absolute magnitude of dimensionless deflection increases as a matter of fact that increasing the material gradient index the stiffness of the FG microbeam decreases. It occurs as a sudden change in the responses when the material gradient index varies from 0 to 5, all of the curves become flatter after passing $p$ = 5. The magnitude of deflection for C-C boundary condition is smaller than that of S-S condition because of the stronger constraints provided by C-C boundary condition. Meanwhile, the maximum value of dimensionless deflection is nearer to −2.7 and −2.3 for SS and CC boundary conditions, respectively.

The effect of the thermal loading on the dimensionless deflection of FG microbeam ($L/h$ = 10) for different material gradient indexes is presented in figure 3. As seen from this figure, it is affirmed that increase in the thermal loading results in the increase of the absolute magnitude of dimensionless deflection. Therefore, it can be said that increasing in thermal loading on FG microbeam decreases its stiffness.

The influence of Winkler foundation on the dimensionless deflection of FG microbeam with several values of the nonlocal parameter is studied in figure 4. It is found that an increase Winkler foundation yields constant magnitude in the stiffness of the FG microbeam. Further,

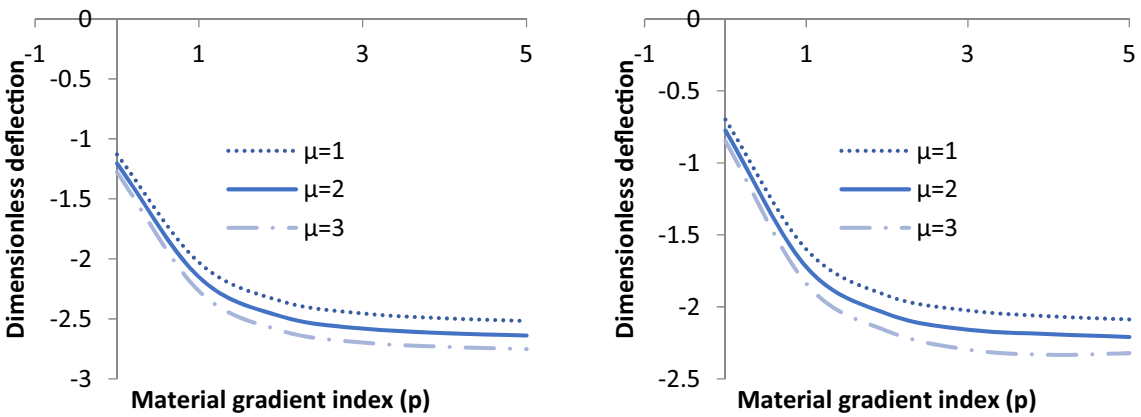


**Figure 2.** Dimensionless deflection versus the material gradient index for various nonlocal parameter (L/$h$=10, $\Delta T$=20, $\Delta H$=1, $K_w$= $K_p$=20).

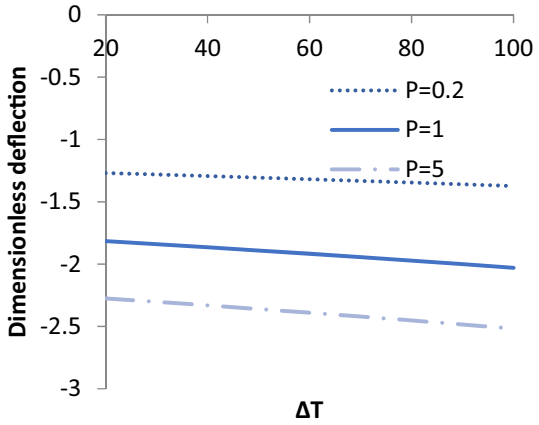


**Figure 3.** Dimensionless deflection versus the temperature rise for various material gradient index $L/h$=10, $\mu$=1, $\Delta H$=1, $K_w$= $K_p$=20).

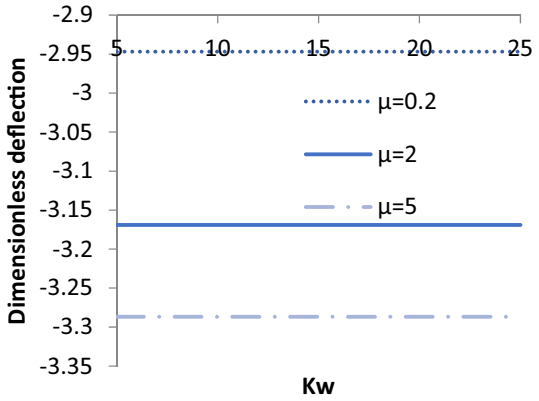


**Figure 4.** Dimensionless deflection versus the Winkler coefficient for various and various nonlocal parameters ( $L/h$=10, p=5, $\Delta H$=1, $K_p$=20).

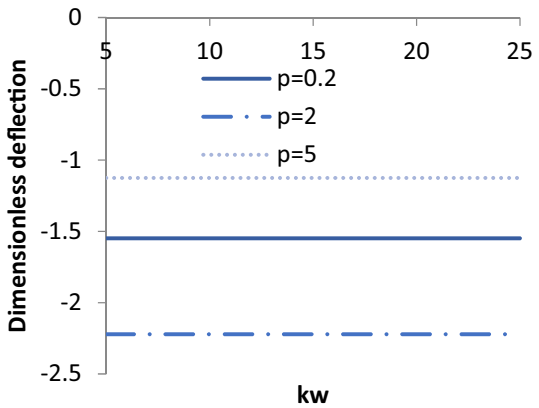


**Figure 5.** Dimensionless deflection versus the Winkler coefficient for various and various material gradient index parameters ($L/h$=10, $\mu$=1, $\Delta H$=1, $K_p$=20).

it is also evident from this figure that when nonlocal parameter increases the absolute magnitude of dimensionless deflection increases.

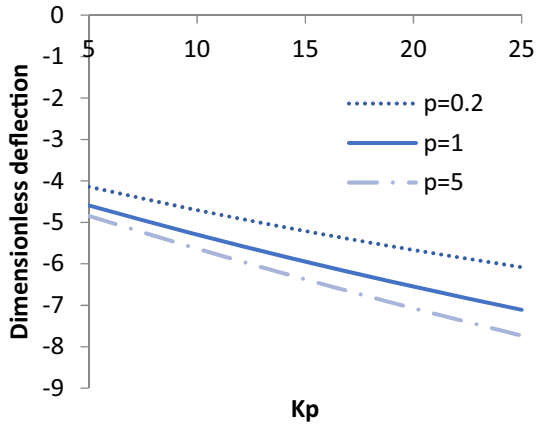


**Figure 6.** Dimensionless deflection versus the Pasternak coefficient for various and various material gradient index parameters ( $L/h$=10, $p$-5, $\Delta H$=1, $K_w$=20).

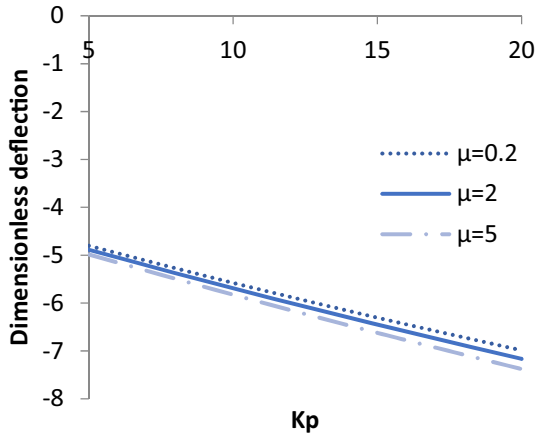


**Figure 7.** Dimensionless deflection versus the Pasternak coefficient for various and various nonlocal parameters ( $L/h$=10, $\mu$=1, $\Delta H$=1, $K_w$=20).

Figure 5 illustrates the influence of Winkler foundation associated with serval values of the material gradient index, on the dimensionless deflection of FG microbeam. It can be noticed from this figure that any improvement in the Winkler coefficient has a negligible effect on the dimensionless deflection. In other words, the dimensionless deflection remains constant with an increase in the Winkler coefficient.

The influence of the Pasternak foundation on the absolute magnitude of dimensionless deflection of FG microbeam for various values of the nonlocal parameter is shown in figure 6. It can be noticed from this evaluation that unlike Winkler coefficient, the Pasternak coefficient has a significant influence on the dimensionless deflection. To be specific, the absolute magnitude of dimensionless deflection increases with the increase in the Pasternak coefficient. In addition, the deflections decrease as the nonlocal parameter increases.

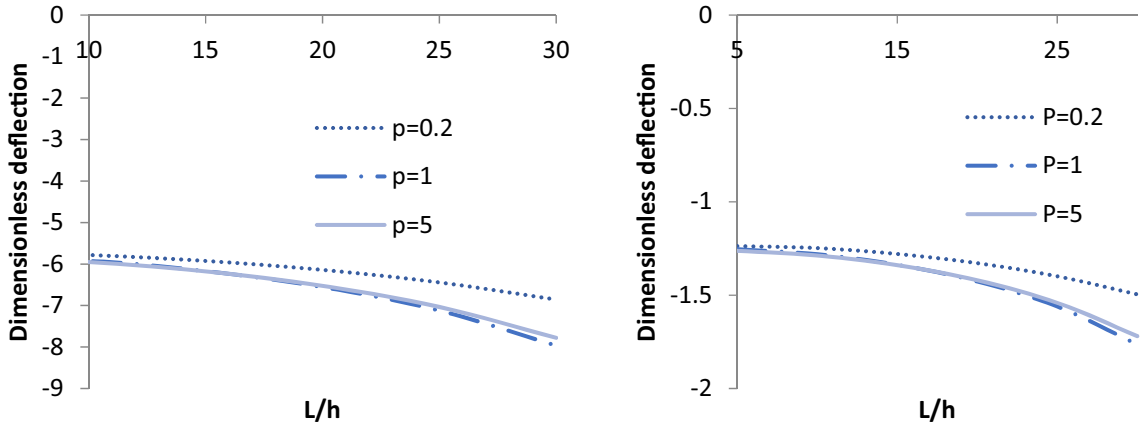


**Figure 8.** Dimensionless deflection versus aspect ratio for various material gradient index parameters ($p$=5, $\mu$=1, $\Delta H$=1, $K_p$ =$K_w$=20).

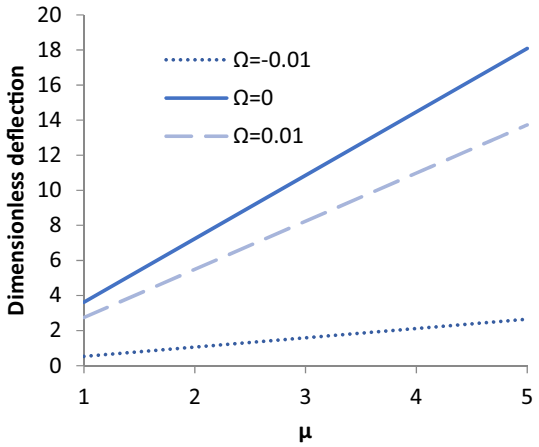


**Figure 9.** Effect of nonlocal parameters on dimensionless deflection for uniform load for various magnet potential parameter (L/$h$=10, $V$=0,$K_w$= $K_p$=20,ΔT=20,ΔH=1).

The study is extended to assess the effect of the Pasternak foundation on the dimensionless deflection of FG microbeam with various values of the nonlocal parameter, as shown in figure 7. It can be witnessed that the absolute magnitude of dimensionless deflection increases when the pasternak coefficient increases. Further as the nonlocal parameter improves the absolute magnitude of dimensionless deflection increases.

Figure 8 shows the dimensionless deflection of FG microbeam with different aspect ratios. The nonlocal parameter μ = 1 nm is considered. In this example, the aspect ratio varies from $L/h$ = 10 to $L/h$ = 30. This result indicates that the effect of aspect ratio softens the microbeam. In addition, the maximum deflection increases with increasing the material gradient index of the microbeam.

Figure 9 investigates the effect of nonlocal parameter on the dimensionless deflection of FG microbeam applied with various magnet potential. It can be witnessed that higher value of nonlocal parameter yields a higher dimensionless deflection. Further, the results also reveal that increasing the value of magnet potential from negative magnitude to the positive magnitude results in the increase of dimensionless deflection. Therefore, the magnet potential has a significant role in analyzing the deflection.

The effect of slenderness ratio on the deflection of FG microbeam is shown in figure 10. Also the influence of external voltage is evaluated. It can be seen that for negative voltages, as the slenderness ratio increases the deflection increases whereas for positive voltage, improvement in the slenderness ratio reduces the deflection. This is due to the axial tensile and compressive forces produced in the microbeams via the constructed positive and negative voltages, respectively. In addition, it is lightly observed that the dimensionless deflection is approximately independent of slenderness ratio for zero electric voltages ($V = 0$).

The variations of the dimensionless deflection of microbeams versus the Winkler and Pasternak parameters for various electric voltages at L/h=10 are shown in figure 11. It is found from this figure that regardless of the sign and magnitude of electric voltage, the dimensionless deflection increases with the increase of Winkler and Pasternak parameters. Therefore, the stiffness of the microbeam reduces. It must be mentioned that at a constant electric voltage the increase of dimensionless deflection with Pasternak parameter measurement with a higher rate than those of Winkler parameter.

The effect of the aspect ratio versus the dimensionless deflection of microbeam for various values of Winkler foundations shown in figure 12. One can observe that the dimensionless static deflections increase from L/h=10–20 after that the deflection decreases with the increase of aspect ratio. It may be

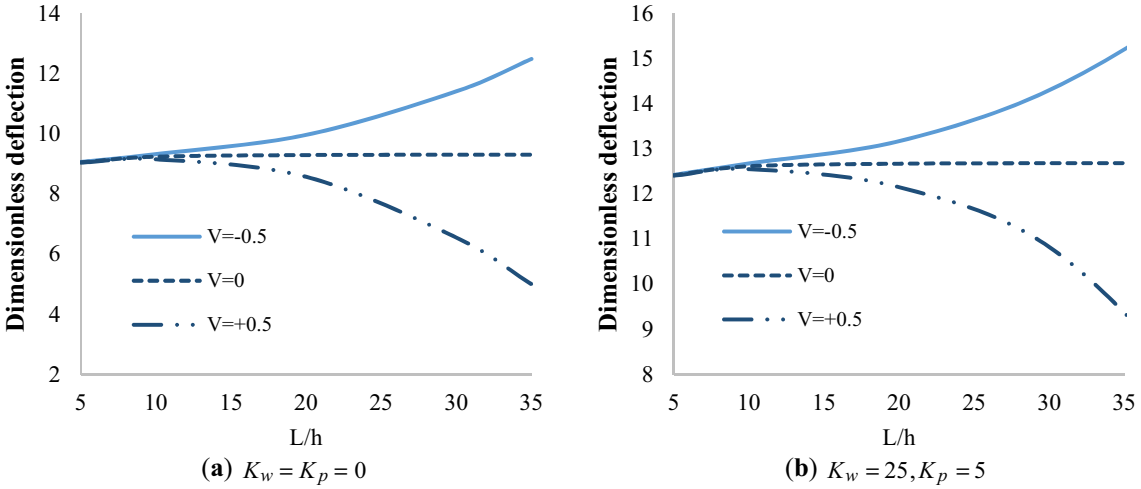


**(a)** $K_w = K_p = 0$ **(b)** $K_w = 25, K_p = 5$

**Figure 10.** Effect of slenderness ratio dimensionless deflection for uniform load for various of electric voltage with voltage without elastic foundation and with elastic foundation (L/*h*=10, Ω=*0*,ΔT=20,ΔH=1).

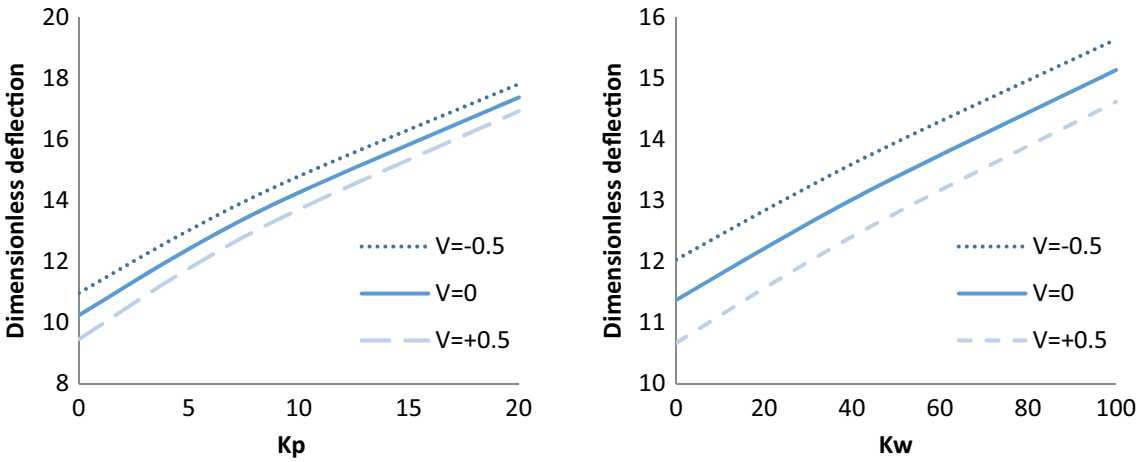


**Figure 11.** Effect of the Pasternak foundation on dimensionless deflection for uniform load and various electric voltage ($L/h$=10,$K_w$=$K_p$=20,$\mu = 2, \Omega = 0, \Delta T = 20, \Delta H = 1$).

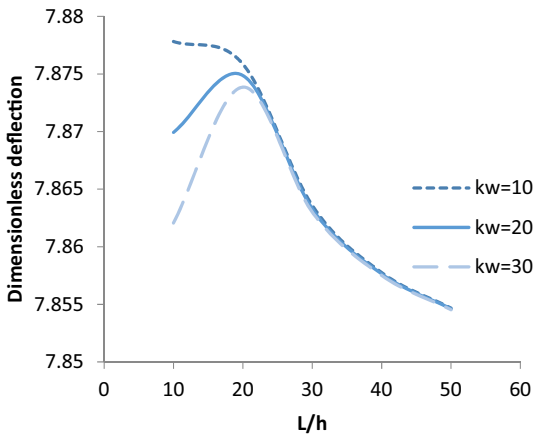


**Figure 12.** Effect of aspect ratio on dimensionless deflection for uniform load and various Winkler foundation ($L/h$=10, $K_p$=20,$V = 0, \Omega = 0, \Delta T = 20, \Delta H = 1$).

due to the fact that an increase of Winkler foundation yields increase magnitude in the stiffness of the microbeam.

## 5. Conclusions

The present article evaluates the dimensionless deflection of flexoelectricity FG microbeams resting on Winkler-Pasternak foundation under hygro-thermal loading. To this end, an analytical formulation is proposed through higher order refined beam theory. The foundation includes Winkler-Pasternak layer. Hamilton's principle is used to obtain the governing equations based on the nonlocal theory and solved administrating an analytical solution. The effects of Winkler, Pasternak foundation, flexoelectricity, hygro-thermal environment, nonlocal

parameter, material gradient index on the deflection of piezoelectric FG microbeams are verified. The results reveal that an increment in the material gradient index, nonlocal parameter and thermal loading yields a higher absolute magnitude of dimensionless deflection. Meanwhile, the Winkler coefficient has a negligible influence on the deflection whereas Pasternak coefficient significantly affects the bending behaviour of FG microbeam. Further, as the aspect ratio increases the deflections improve.

## References


[1] Eringen A 1968 Mechanics of micromorphic continua. In: *Mechanics of Generalized Continua*. Springer, Berlin, Heidelberg, pp 18–35

[2] Eringen A 1972 Nonlocal polar elastic continua. *Int. J. Eng. Sci.* 10: 1–16

[3] Ansari R, Pourashraf T and Gholami R 2015 An exact solution for the nonlinear forced vibration of functionally graded nanobeams in thermal environment based on surface elasticity theory. *Thin Walled Struct.* 93: 169–176

[4] Kiani Y, Rezaei M, Taheri S, Eslami M R 2011 Thermo-electrical buckling of piezoelectric functionally graded material Timoshenko beams. *Int. J. Mech. Mater. Des.* 7: 185–197

[5] Rahmani O and Jandaghian A A 2015 Buckling analysis of functionally graded nanobeams based on a nonlocal third-order shear deformation theory. *Appl. Phys. A.* 119: 1019–1032

[6] Yang J, Ke L L and Kitipornchai S 2010 Nonlinear free vibration of single-walled carbon nanotubes using nonlocal Timoshenko beam theory. *Physica E: Low-dimensional Systems and Nanostructures.* 42: 1727–1735

[7] Ebrahimi F and Barati M R 2016 Dynamic modeling of a thermo–piezo-electrically actuated nanosize beam subjected to a magnetic field. *Appl. Phys. A.* 122: 1–18

[8] Ebrahimi F and Barati M R 2016 Electromechanical buckling behavior of smart piezoelectrically actuated higher-order size-dependent graded nanoscale beams in thermal environment. *Int. J. Smart Mater. Nano Struct.* 7(2): 69–90

[9] Ebrahimi F and Barati M R 2016 An exact solution for buckling analysis of embedded piezoelectro-magnetically actuated nanoscale beams. *Adv. Nano Res.* 4(2): 65–84

[10] Ebrahimi F and Barati M R 2018 Vibration analysis of smart piezoelectrically actuated nanobeams subjected to magneto-electrical field in thermal environment. *J. Vib. Control.* 24(3): 549–564

[11] Ebrahimi F and Barati M R 2017 Buckling analysis of nonlocal third-order shear deformable functionally graded piezoelectric nanobeams embedded in elastic medium. *J. Braz. Soc. Mech. Sci. Eng.* 39: 937–952

[12] Roque C M C, Ferreira A J M and Reddy J N 2011 Analysis of Timoshenko nanobeams with a nonlocal formulation and meshless method. *Int. J. Eng. Sci.* 49: 976–984

[13] Peddieson J, Buchanan G R and McNitt R P 2003 Application of nonlocal continuum models to nanotechnology. *Int. J. Eng. Sci.* 41: 305–312

[14] Civalek O and Demir C 2011 Bending analysis of microtubules using nonlocal Euler-Bernoulli beam theory. *Appl. Math, Model.* 35: 2053–2067

[15] Wang Q 2005 Wave propagation in carbon nanotubes via nonlocal continuum mechanics. *J. Appl. Phys.* 98: 124301

[16] Wang C M, Kitipornchai S, Lim C W and Eisenberger M 2008 Beam bending solutions based on nonlocal Timoshenko beam theory. *J. Eng. Mech.* 134: 475–481

[17] Murmu T and Pradhan S C 2009 Buckling analysis of a single-walled carbon nanotube embedded in an elastic medium based on nonlocal elasticity and Timoshenko beam theory and using DQM. *Physica E: Low-dimensional Systems and Nanostructures.* 41: 1232–1239

[18] Arefi M and Zenkour A M 2016 A simplified shear and normal deformations nonlocal theory for bending of functionally graded piezomagnetic sandwich nanobeams in magneto-thermo-electric environment. *J. Sandw. Struct. Mater.* 18: 624–651

[19] Zenkour A M and Sobhy M 2013 Nonlocal elasticity theory for thermal buckling of nanoplates lying on Winkler-Pasternak elastic substrate medium. *Physica E: Low-dimensional Systems and Nanostructures.* 53: 251–259

[20] Ghorbanpour Arani A and Zamani M H 2019 Investigation of electric field effect on size-dependent bending analysis of functionally graded porous shear and normal deformable sandwich nanoplate on silica Aerogel foundation. *J. Sandw. Struct. Mater.* 21(8): 2700–2734

[21] Şimşek M and Yurtcu H H 2013 Analytical solutions for bending and buckling of functionally graded nanobeams based on the nonlocal Timoshenko beam theory. *Compos. Struct.* 97: 378–386

[22] Tornabene F 2009 Free vibration analysis of functionally graded conical, cylindrical shell and annular plate structures with a four-parameter power-law distribution. *Comput Method Appl. Mech. Eng.* 198: 2911–2935

[23] Zghal S, Frikha A and Dammak F 2018 Mechanical buckling analysis of functionally graded power-based and carbon nanotubes-reinforced composite plates and curved panels. *Compos. Part B: Eng.* 150: 165–183

[24] Tornabene F, Liverani A and Caligiana G 2011 FGM and laminated doubly curved shells and panels of revolution with a free-form meridian: a 2-D GDQ solution for free vibrations. *Int. J. Mech. Sci.* 53: 446–470

[25] Frikha A, Zghal S and Dammak F 2018 Dynamic analysis of functionally graded carbon nanotubes-reinforced plate and shell structures using a double directors finite shell element. *Aerosp. Sci. Technol.* 78: 438–451

[26] Tornabene F and Reddy J N 2013 FGM and laminated doubly-curved and degenerate shells resting on nonlinear elastic foundations: a GDQ solution for static analysis with a posteriori stress and strain recovery. *J. Indian Inst. Sci.* 93: 635–688

[27] Trabelsi S, Frikha A, Zghal S and andDammak F, 2019 A modified FSDT-based four nodes finite shell element for thermal buckling analysis of functionally graded plates and cylindrical shells. *Eng. Struct.* 178: 444–459

[28] Tornabene F, Fantuzzi N, Viola E and Batra R C 2015 Stress and strain recovery for functionally graded free-

form and doubly-curved sandwich shells using higher-order equivalent single layer theory. *Compos. Struct.* 119: 67–89

[29] Tornabene F, Fantuzzi N, Bacciocchi M and Viola E 2016 Effect of agglomeration on the natural frequencies of functionally graded carbon nanotube-reinforced laminated composite doubly-curved shells. *Compos. Part B: Eng.* 89: 187–218

[30] Ebrahimi F and Salari E 2016 Effect of various thermal loadings on buckling and vibrational characteristics of nonlocal temperature-dependent FG nanobeams. *Mech. Adv. Mater. Struct.* 23: 1379–1397

[31] Sobhy M 2013 Buckling and free vibration of exponentially graded sandwich plates resting on elastic foundations under various boundary conditions. *Compos. Struct.* 99: 76–87

[32] Ebrahimi F and Salari E 2015 Thermo-mechanical vibration analysis of nonlocal temperature-dependent FG nanobeams with various boundary conditions. *Compos. Part B: Eng.* 78: 272–290

[33] Berrabah H M, Tounsi A, Semmah A and Adda B 2013 Comparison of various refined nonlocal beam theories for bending, vibration and buckling analysis of nano-beams. *Struct. Eng. Mech.* 48: 351–365